

Computer problems

to Lecture Notes on:

Fundamentals of Atmospheres and Oceans on Computers

Lars Petter Røed
Norwegian Meteorological Institute
P. O. Box 43 Blindern
0313 Oslo, Norway

and

Department of Geosciences
University of Oslo
Section Meteorology and Oceanography
P. O. Box 1022 Blindern
0315 Oslo, Norway

Fall 2011

Printed
November 16, 2011

PREFACE

Presented is a set of computer problems to go with the lecture notes on “Fundamental of Atmospheres and Oceans on Computers”. Four of these are compulsory and must be submitted for evaluation. The students may, to a certain degree, decide which problems to turn in themselves. The mandatory problems replace the mid term exam. Four of the problems must be approved before the student is allowed to take the (oral) exam.

Solving atmospheric and oceanographic problems, sometimes referred to as metocean problems, using numerical methods consist of four stages. The first is to develop a numerical analogue of the continuous mathematical problem formulated based on the physical problem at hand. The second is to construct and run a computer code (or program) on a given computer. This stage includes debugging and verification. Debugging means to check that the code has no formal errors, and that the code is a true replica of the numerical analogue. Verification is a bit harder. It implies checking the results against what is known about the true solution, e.g., analytic solutions. The final and third stage is to be able to visualize the results, and finally to discuss them in light of what physics the solution represent. All three stages are equally important.

I strongly recommend all students to solve as many of the problems as possible in order to get the necessary hands-on experience and insight into stages two and three.

The problems will be continuously amended to adjust to the lecture notes. The author would like to thank the many colleagues who has contributed to the development of these exercises over the years, and to the many students for pointing out misprints and other mistakes.

Good luck!

Blindern, September 19, 2011

Lars Petter Røed (sign.)

Revision history (most recent on top):

All revisions made by the author.

- ☞ Nov 07, 2011: The problem set “Geostrophic adjustment - planetary waves” is split in two. One is called “Geostrophic adjustment” and is found in Problem set 6. The second is called “Planetary waves” and is found in Problem set 8.
- ☞ Oct 17, 2011: Made changes and correction to the Problem set: Advection in the Atmosphere and Ocean
- ☞ Sep 19, 2011: A new Problem set 3 is ammended which is a coupled atmosphere-ocean diffusion problem
- ☞ Sep 19, 2011: The starting point is the set of Computer problems for the fall of 2010, which in turn is based on earlier versions

Contents

PREFACE	ii
1 Problem set: Truncation errors	1
2 Problem set: Vertical Diffusive Mixing	2
3 Problem set: Vertical Mixing in a coupled Atmosphere-Ocean	5
4 Problem set: Yoshida's equatorial jet current	9
5 Problem set: Advection in the Atmosphere and Ocean	12
6 Problem set: Geostrophic Adjustment	16
7 Problem set: Flux correction methods	21
8 Problem set: Planetary waves	23
9 Problem set: Rossby waves	27
10 Problem set: Storm surges	31
11 Problem set: Method of characteristics	37
12 Problem set: Upwelling in the Bay of Guinea	38
REFERENCES	41

List of Figures

1	Left-hand panel displays the initial temperature distribution according to (8), while the right-hand panel shows the time evolution of the surface temperature according to (11) and (12), respectively.	4
2	Depicted is the initial potential temperature distribution according to (22) and the time evolution of the potential temperature as time progresses for five time levels.	7
3	Sketch of a reduced gravity ocean model consisting of two layers with a density difference given by $\Delta\rho$	9
4	This is the solution for the initial wide bell function using the leapfrog scheme with $C = 0.5$	14
5	Depicted is the initial geopotential height according to (52).	18
6	Sketch of a storm surge model along a straight coast conveniently showing some of the notation used.	32
7	Displayed is the cell structure of lattice B of <i>Mesinger and Arakawa (1976)</i> in one space dimension. The circels are associated with h -points, while the horizontal bar is associated with U -points and the vertical bar with V -points within the same cells. The sketched staggering is such that the distance between adjacent h -points and U, V -points are one half grid distance apart.	35
8	Sketch of the model domain for which (114) and (115) is to be solved.	39
9	Skisse av vindstresset	40
10	Speiling av hastighetspunketer ved faste render i et forskjøvet gitter. Sirkler, (O), angir h -punkter, horisontale streker, (—), u -punkter, mens vertikale streker, , angir et v -punkt.	41

1 Problem set: Truncation error in a recursion formula with two terms

a.

Let

$$\pi = 4 \arctan(1), Z_1 = \pi, \text{ and } S_1 = \pi. \quad (1)$$

Compute

$$Z_{i+1} = 3.1Z_i - 2.1Z_1 \text{ and } S_{i+1} = \left(\frac{9.}{5.}\right) S_i - \left(\frac{4.}{5.}\right) S_1 \quad (2)$$

for $i = 1(1)100$. Compute also the *relative* error (e.g., $\epsilon_i = Z_{i+1} - Z_i/Z_i$) for each i . Write π , Z_i , S_i and the relative error in percent. The output should be readable and self explanatory, e.g., should have headings for each column. Enclose the program code and the printout when you turn in your paper. Do the problem on different platforms (from handholds to portables, PCs and supercomputers) available to you. Experiment by using different constants in the recursion formulas. Does it make a difference in the answer?

The purpose of the exercise is twofold: 1) It is simple enough to enable you to refresh your knowledge of FORTRAN or FORTRAN skills without having to write lengthy codes, and 2) it demonstrates the dramatic consequences of the presence of insignificant truncation errors always present in numerical computations.

b.

Show analytically why the recursion formulas for Z_i and S_i do not compute π correctly.

2 Problem set: Vertical Diffusive Mixing

In the ocean and atmosphere the vertical (and horizontal) heat exchange is dominantly a turbulent process. Commonly the vertical turbulent heat exchange is parametrized as a diffusion process, that is, governed by the equation

$$\partial_t \theta + \partial_z F = 0, \quad (3)$$

where $\theta = \theta(z, t)$ is the potential temperature, z is the vertical coordinate, t is time and F is the vertical component of the diffusive flux vector.

In its simplest form the heat exchange is parametrized as a down the gradient diffusion process. Thus

$$F = -\kappa \partial_z \theta, \quad (4)$$

where κ is the diffusion coefficient, and (3) becomes

$$\partial_t \theta = \partial_z (\kappa \partial_z \theta). \quad (5)$$

Note that since the heat exchange is due to turbulent mixing the diffusion or mixing coefficient κ is normally a function of space and time. We underscore that θ can be any active tracer like temperature, humidity and salinity, or a passive tracer like CO_2 .

In this exercise we assume that the diffusion coefficient is constant. Under these circumstances (5) reduces to

$$\partial_t \theta = \kappa \partial_z^2 \theta. \quad (6)$$

You are asked to solve (6) numerically for two applications. The first is associated with mixing in the atmospheric planetary boundary layer, while the second is associated with mixing in the oceanic mixed layer. The mixing or diffusion coefficient in the two spheres are dramatically different. While the mixing coefficient for the atmospheric boundary layer is $\kappa = 30 \text{ m}^2\text{s}^{-1}$, the similar mixing coefficient for the oceanic mixed layer is a factor 10^{-4} less, namely $\kappa = 3 \cdot 10^{-3} \text{ m}^2\text{s}^{-1}$ (Gill, 1982).

In this exercise we assume that the fluid is contained between two fixed z -levels, where the boundary conditions replace (6). Regarding the atmospheric application we assume that the bottom level is located at $z = 0$, while the top level $z = D$ is at the top of the planetary mixed layer. For the ocean application the bottom level is the mixed layer at depth $z = -D$ while the top level is the surface at $z = 0$. Thus $z \in \langle 0, D \rangle$ for the atmospheric application and $z \in \langle -D, 0 \rangle$ for the oceanic application. For both cases you are asked to find the numerical solution for $t \in [0, N\Delta t]$ where $N = 401$, that is, $t = n\Delta t, n = 0(1)N$, where n is the time step counter, Δt is the time step and N is the total number of time levels. We assume that the mixed layers are $D = 100 \text{ m}$ deep in both cases. Furthermore we let $D = (J_{max} - 1)\Delta z$ where Δz is the space increment¹ and $J_{max} = 27$ is the total number of grid points including the two boundary points at the bottom and top levels.

¹Also commonly referred to as the mesh or grid size.

a.

Develop a numerical scheme (or finite difference approximation) that is forward in time and centered in space for (6). Show that the derived scheme is stable under the condition $K \leq \frac{1}{2}$, where

$$K = \frac{\kappa \Delta t}{\Delta z^2}. \quad (7)$$

b.

Next develop a finite difference approximation for (6) that is centered in both time and space, and show that this algorithm is unconditionally unstable in a numerical sense.

c.

Let $K = 0.45$. Compute the time step you will have to use for the atmospheric and oceanic applications, respectively. Discuss why there is such a huge difference and its possible consequences.

d.

Consider first an atmospheric application. We assume that initially the temperature distribution is a sinusoidal function of height as shown in the left-hand panel of Figure 1. Thus we assume

$$\theta(z, 0) = \theta_0 \sin\left(\frac{\pi z}{D}\right), \quad z \in [0, D], \quad (8)$$

where $\theta_0 = 10^\circ\text{C}$. Furthermore we let the temperature at the bottom level (or surface) $z = 0$ and the top level $z = D$ be fixed at the freezing point for all times, that is,

$$\theta(0, t) = \theta(D, t) = 0^\circ\text{C} \quad \forall t. \quad (9)$$

Use the stable forward in time, centered in space scheme developed under a. to find the numerical solution to (6) for two cases; one with $K = 0.45$ and a second with $K = 0.55$. Plot the results for $n = 0$, $n = 50$, $n = 100$ and $n = 200$ in which the height and temperature are made dimensionless by dividing through by D and θ_0 , respectively.

Derive the analytic solution to (6) given the initial condition (8) and the boundary conditions (9). Assess and discuss the solutions by comparing the numerical and analytic solutions. Explain in particular why the solution for $K = 0.55$ develops a “saw tooth” pattern.

e.

Consider next an oceanographic application. In this case we assume that the initial condition is

$$\theta(z, 0) = 0^\circ\text{C}, \quad z \in [-D, 0], \quad (10)$$

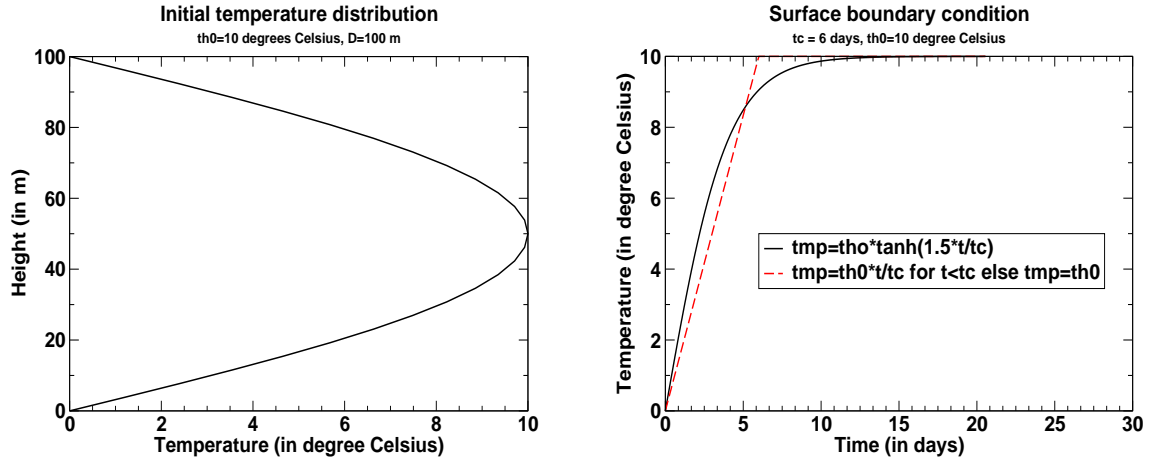


Figure 1: Left-hand panel displays the initial temperature distribution according to (8), while the right-hand panel shows the time evolution of the surface temperature according to (11) and (12), respectively.

throughout the water column. Thus the initial condition is the trivial solution to (6). In contrast to the atmospheric application the diffusion process is generated by letting the ocean surface be heated from above. Specifically, we let the boundary condition at $z = 0$ increase from zero to a fixed temperature $\theta_0 = 10^\circ\text{C}$ after some finite time. This can be achieved either by letting the boundary condition be specified according to

$$\theta(0, t) = \theta_0 \begin{cases} \frac{t}{t_c} & ; 0 < t < t_c \\ 1 & ; t \geq t_c \end{cases}, \quad (11)$$

where $t_c = 6$ days determines how fast the surface temperature reaches its final temperature θ_0 (cf. the right-hand panel of Figure 1), or by using a hyperbolic tangent (a good function), that is,

$$\theta(0, t) = \theta_0 \tanh\left(\frac{\gamma t}{t_c}\right) \quad (12)$$

where $\gamma = 1.5$ together with t_c determines how fast the temperature approaches its final temperature (cf. the right-hand panel of Figure 1). At the bottom of the ocean mixed layer $z = -D$ the temperature is fixed at the freezing point. Thus

$$\theta(-D, t) = 0^\circ\text{C} \quad (13)$$

Again choose the time step so that $K = 0.45$. Plot the results for $n = 0$, $n = 100$, $n = 200$ and $n = 400$. Use either (11) or (12) as your surface boundary condition.

Assess and discuss the solution. In particular you are asked to compare the solution with the steady state solution to (6), that is, the solution as $t \rightarrow \infty$ given the above initial and boundary conditions.

3 Problem set: Vertical Mixing in a coupled Atmosphere-Ocean

In the ocean and atmosphere the vertical (and horizontal) exchange or flux of a tracer is dominantly a turbulent process. In its simplest form the vertical turbulent mixing flux, say F , is commonly parametrized as a down the gradient diffusion process, that is,

$$F = -\kappa\partial_z\theta, \quad (14)$$

where θ is the tracer, z is the vertical coordinate and κ is the efficiency of the mixing. In (14) the mixing is parameterized as diffusion, in which case it is common to refer to κ as the diffusion coefficient. If vertical mixing is the only active physical process, then the time rate of change of the tracer is governed by the equation

$$\partial_t\theta + \partial_z F = 0, \quad (15)$$

where t is time. Substituting (14) in (15) we get

$$\partial_t\theta = \partial_z(\kappa\partial_z\theta). \quad (16)$$

We underscore that θ can be any active tracer like potential temperature, humidity and salinity, or a passive tracer like CO_2 . We also note that κ depends on the motion, and hence is a function of space and time. Nevertheless, we assume that the diffusion coefficient is constant below. We emphasize though that the mixing coefficient in the atmospheric boundary layer (ABL) and the oceanic mixed layer (OML) is dramatically different. While the mixing coefficient in the ABL is $\kappa_A = 30 \text{ m}^2\text{s}^{-1}$, the similar mixing coefficient in the OML is a factor 10^{-4} less, namely $\kappa_O = 3 \cdot 10^{-3} \text{ m}^2\text{s}^{-1}$ (Gill, 1982). We must therefore solve (16) separately in the the two spheres, that is,

$$\partial_t\theta = \begin{cases} \kappa_A\partial_z^2\theta; & z \in \langle 0, D \rangle, \\ \kappa_O\partial_z^2\theta; & z \in \langle -H, 0 \rangle, \end{cases} \quad (17)$$

where $z = D$ is the top level of the ABL and $z = -H$ is the bottom level of the OML.

In this Problem set we consider θ to be potential temperature. You are asked to solve (17) numerically for the time span $t \in \langle 0, T \rangle$. In solving (17) we let the atmosphere and the ocean span the vertical space $z \in [-H, D]$, where $D = 270\text{m}$ and $H = 30\text{m}$ are constants, and let the interface between them be located at $z = 0$. To solve (17) we need four boundary conditions in space and one initial condition in time. In all cases below the initial condition is as specified in (22) below. At the top and bottom of the respective mixed layers we assume that the potential temperatures are fixed as time progresses, except for one case below (cf. item **i.** below) in which we require the top of the ABL to be insulated. In the former case we hence assume $\theta = \theta_T = 0^\circ\text{C}$ at $z = D$ and $\theta = \theta_B = 10^\circ\text{C}$ at $z = -H$ (Dirichlet boundary conditions), while in the latter case we require the heat flux to be zero at the top of the ABL (a Neuman condition) as given by (23) below. At the interface we require that the heat fluxes and the tracer itself is continuous, that is,

$$\kappa_A\partial_z\theta|_{z \rightarrow 0^+} = \kappa_O\partial_z\theta|_{z \rightarrow 0^-} \quad \text{and} \quad \theta|_{z \rightarrow 0^+} = \theta|_{z \rightarrow 0^-}. \quad (18)$$

a.

Please explain why we need four boundary conditions in space and one in time?

b.

Show that a stationary solution to (17) exists and is given by

$$\theta = \begin{cases} \kappa_O \gamma (z - D) + \theta_T & z \in [0, D], \\ \kappa_A \gamma (z + H) + \theta_B & z \in [-H, 0), \end{cases} \quad (19)$$

where

$$\gamma = \frac{\theta_T - \theta_B}{\kappa_A H + \kappa_O D}. \quad (20)$$

c.

Develop a numerical scheme or finite difference equation that is forward in time and centered in space (an FTCS scheme) to replace the continuous equations (17). Show that the derived scheme is stable under the conditions $K_A \leq \frac{1}{2}$ and $K_O \leq \frac{1}{2}$, where

$$K_A = \frac{\kappa_A \Delta t_A}{\Delta z_A^2} \quad \text{and} \quad K_O = \frac{\kappa_O \Delta t_O}{\Delta z_O^2}. \quad (21)$$

Here Δt_A and Δt_O are the time steps of the atmospheric and oceanic parts, respectively, while Δz_A and Δz_O are the respective space increments. The latter is also referred to as the mesh size or grid size.

d.

Show that $D = J_A \Delta z_A$ and $H = J_O \Delta z_O$. Furthermore let $J_A = J_O = 27$ and $K_A = K_O = 0.45$. Compute the time steps you will have to use for the atmospheric and oceanic parts, respectively, and discuss why there is such a huge difference in the time steps. Please also discuss its possible consequences in terms of physics and numerics.

e.

If we require $K_O = K_A = 0.45$ then either Δt_O or Δz_O has to change. From a numerical point of view it is advantageous to let Δz_O change. Please explain why.

f.

Show that if we let $\Delta t_A = \Delta t_O$ and $K_O = K_A = 0.45$ then J_O becomes equal to 300 implying that $\Delta z_O = 0.1\text{m}$. Next compute K_O under the condition that $\Delta t_A = \Delta t_O$ and $J_O = J_A = 27$. Does it satisfy the sufficient condition for stability? In the latter case discuss its implications for the growth factor.

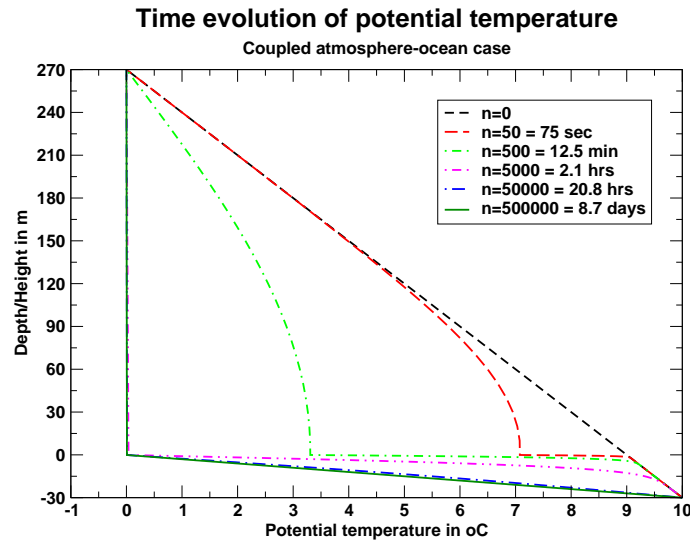


Figure 2: Depicted is the initial potential temperature distribution according to (22) and the time evolution of the potential temperature as time progresses for five time levels.

g.

Initially we assume that the potential temperature distribution is linear in both spheres as depicted in Figure 2. Thus we assume,

$$\theta(z, 0) = -\frac{\theta_B - \theta_T}{H + D}(z - D) + \theta_T, \quad z \in [-H, D]. \quad (22)$$

The initial heat flux is hence discontinuous at the interface.

Use the FTCS scheme developed in item **a.** to find the numerical solution to (17) for two cases; a stable case in which $K_A = 0.45$ and a second unstable case in which $K_A = 0.55$. Plot the results for the stable case for $n = 0$ (initial distribution), $n = 50$, $n = 500$, $n = 5000$, $n = 50000$ and $n = 500000$. Plot the results for the unstable case for $n = 0$, $n = 10$, $n = 20$, $n = 30$, $n = 40$ and $n = 50$. Compute the time in hours for each case, and put it in the legend.

Please keep the scale along the axes in the two cases so that the potential temperature range is $\theta \in [\theta_B, \theta_T]$ and the depth/height range is $z \in [-H, D]$. Preferably the plot should show the height/depth along the vertical axis and the potential temperature along the horizontal axis as shown in the right-hand panel of Figure 2, which also conveniently shows the results for the stable case.

h.

Assess and discuss the solution. In particular you are asked to compare the solution with the steady state solution to (17), that is, the solution as $t \rightarrow \infty$ given the above initial and boundary conditions. Explain in particular why the solution for $K_A = 0.55$ develops a “saw tooth” pattern.

i.

What happens if the upper boundary condition is changed to a no flux condition? Note that the no flux condition is,

$$F = -\kappa_A \partial_z \theta = 0 \quad ; \quad z = D, \quad (23)$$

or $\partial_z \theta = 0$ at $z = D$. Thus we replace the former Dirichlet condition at the top of the ABL by a Neuman condition. Plot the results as done in item **e.**

4 Problem set: Yoshida's equatorial jet current

Like *Yoshida* (1959) we consider an “infinite” equatorial ocean consisting of two immiscible layers with a density difference $\Delta\rho$ (Figure 3). The density of the lower layer equals the reference density ρ_0 . The lower layer is thick with respect to the upper layer. At time $t = 0$ the ocean is at rest, at which time the thickness of the upper layer equals its equilibrium depth H . At this particular time the ocean is forced into motion by turning on a westerly wind (wind from the west).

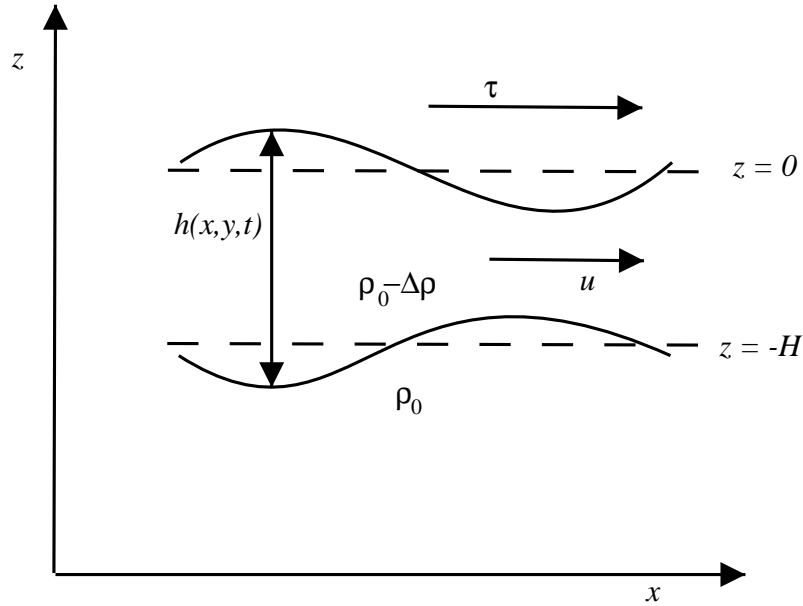


Figure 3: Sketch of a reduced gravity ocean model consisting of two layers with a density difference given by $\Delta\rho$.

The governing equations of such a “reduced gravity” model of the ocean, is

$$\partial_t u - \beta y v = \frac{\tau^x}{\rho_0 H} \quad (24)$$

$$\partial_t v + \beta y u = -g' \partial_y h \quad (25)$$

$$\partial_t h + H \partial_y v = 0 \quad (26)$$

Here $u = u(y, t)$ and $v = v(y, t)$ are the respectively the east-west and north-south components of the velocity in a Cartesian coordinate system (x, y, z) with x directed eastward along the equator, y directed northwards with $y = 0$ at the equator, and z directed along the negative gravitational direction as displayed in Figure 3. The impact of the Earth's rotation is given by the Coriolis parameter $f = 2\Omega \sin \phi$ where Ω is the Earth's rotation rate and ϕ is the latitude. The westerly wind is given by the wind stress component τ^x which is fixed in time. Furthermore,

we define the reduced gravity by $g' \equiv g(\Delta\rho_0/\rho)$ where g is the gravitational acceleration. The instantaneous thickness of the upper layer is given by $h = h(y, t)$.

Note that at the equator $f = 0$ and that it increases with increasing latitude. A simplified parameterization of this effect is through the so called β -plane approximation,

$$f = \beta y, \quad \text{hvor} \quad \beta = \partial_y f|_{y=0}. \quad (27)$$

We note the β is just a measure of the first term in a Taylor series of f at the equator. Thus it represents the first order effect of the impact of the change in the Earth's rotation rate with latitude.

Part 1:

a.

Show that the inertial oscillation² is eliminated by neglecting $\partial_t v$ in (25).

b.

Show that the system of equations (24) - (26) reduces to the ordinary differential equation

$$L^4 \partial_y^2 v - y^2 v = aLy \quad (28)$$

where

$$L = \sqrt{\frac{c}{\beta}}, \quad a = \frac{\tau^x}{\rho_0 \beta L H}, \quad c = \sqrt{g' H} \quad (29)$$

under the condition that the inertial oscillation is eliminated.

c.

Explain why we are allowed to specify two boundary conditions. In the following we will assume that they are $v|_{y=0} = 0$ and $v|_{y \rightarrow \infty} = 0$.

d.

We make (28) dimensionless by letting $y = L\hat{y}$, $(u, v) = a(\hat{u}, \hat{v})$, and $t = (\beta L)^{-1}\hat{t}$. Use the a direct elliptic solver, e.g., Gauss elimination, to solve the dimensionless expression of (28). Let $\Delta y = 0.1$ and plot \hat{v} and \hat{u} at time $\hat{t} = 1$ as a function of \hat{y} from $\hat{y} = 0$ to $\hat{y} = 8$. We note that $v|_{y \rightarrow \infty} = 0$ and hence that \hat{v} is different from zero at $\hat{y} = 8$. Explain how make use of the condition that $v|_{y \rightarrow \infty} = 0$.

²An oscillation in which the frequency equals the inertial frequency f .

e.

Discuss the numerical solution. Let $\tau^x = 0.1Pa$, $\beta = 2 \cdot 10^{-11}(ms)^{-1}$, $L = 275km$, $\rho = 10^3kgm^{-3}$ and $H = 200m$. What is the maximum current in the equatorial jet for $\hat{t} = 1$?

f.

Solve (28) analytically. Hint: Make a series using Hermitian polynomials (see for instance *Abramowitz and Stegun*, 1965).

5 Problem set: Advection in the Atmosphere and Ocean

Since tracers such as temperature, salinity and humidity has a decisive impact on the dynamics of the atmosphere and ocean through its influence on the pressure distribution through density, advection (transport) of these tracers is of zero order importance to get correct.

Moreover, transport of contaminants in the ocean and atmosphere is one crucial element when discussing environmental issues. For instance emissions of radionuclide in one location are transported via atmospheric and oceanic circulation patterns to quite other locations. Other examples are transboundary advection of chemical substances such as sulfur (mostly atmosphere) and nutrients (mostly ocean). In the ocean advection processes are also of crucial importance regarding search and rescue, oil drift, and drifting objects (e.g, fish larvae, rafts, man overboard, ship wrecks, etc.)

Commonly all transport and spreading of the above are governed by an advection-diffusion equation, say

$$\partial_t \psi + \nabla \cdot (\mathbf{v}\psi) = \nabla \cdot (\kappa \nabla \psi) \quad (30)$$

where ψ is the concentration of the tracer, \mathbf{v} is the three-dimensional wind or current vector and κ is the mixing or diffusion coefficient. We note that commonly the transport is associated with the advection part of (30), while the spreading is associated with the mixing part of (30). While the mixing was exemplified in Computer Problem #s 2 and 3 we focus on the advection part here. Thus we will neglect the mixing part in the remainder of this problem except in the very last question.

To make the problem as simple as possible, but no simpler, we reduce the advection problem to one dimension in space. Furthermore we let the advection speed be constant, say $\mathbf{v} = A\mathbf{i}$, where A is a constant. Thus we will consider numerical solutions to the equation

$$\partial_t \psi + A \partial_x \psi = 0 \quad \text{for } x \in \langle 0, L_x \rangle \quad (31)$$

with appropriate boundary and initial conditions. To this end we will make use of three schemes, namely the *leapfrog scheme*, the *upwind or upstream scheme* and the *Lax-Wendroff scheme*.

Part 1: Analysis

a.

Show that the three schemes are numerically stable under the CFL condition

$$C = |A| \frac{\Delta t}{\Delta x} \leq 1 \quad (32)$$

where C is the Courant number.

b.

Show that a forward in time, centered in space (FTCS) finite difference approximation applied to (31) results in an unconditionally unstable scheme.

c.

Show that the upwind scheme inherently includes a numerical diffusion with a diffusion coefficients given by

$$\frac{1}{2}|A|\Delta x(1 - |C|) \quad (33)$$

where C is the Courant number given in (32).

d.

Let us specify an initial condition at time $t = 0$, that is, let

$$\psi(x, 0) = \psi_0 e^{-\left(\frac{x-x_0}{\sigma}\right)^2} \quad ; \quad \forall x \in [0, L_x], \quad (34)$$

where ψ_0 is the maximum tracer concentration, $x_0 = \frac{1}{2}L_x$ is the position of the initial maximum tracer concentration, and σ is a measure of the width of the bell. Thus the larger σ is, the wider the bell is.

Furthermore let us use a periodic (cyclic) boundary condition in space, that is, let

$$\psi(x, t) = \psi(x + L_x, t). \quad (35)$$

Explain why we cannot specify more or less boundary and/or initial conditions.

e.

By use of the boundary conditions (35) and (34), show that the analytic solution to (31) is

$$\psi(x, t) = \psi_0 e^{-\left(\frac{x-At-x_0}{\sigma}\right)^2}. \quad (36)$$

Note that due to the periodic boundary condition the solution after $t = t_c = L_x/A$ equals the initial condition exactly. The time t_c is henceforth referred to as one cycle.

Part 2: Numerical solutions

Below we asked of you to solve (31) numerically for the domain $x \in [0, L_x]$ where $L_x = 100\text{km}$ is the width of the computational domain. To this end we use the three schemes above. Let $x_j = (j - 1)\Delta x$, $t = n\Delta t$ and let $x = 0$ be associated with $j = 1$, $x = L_x$ with $j = J + 1$ and $t = 0$ with $n = 0$. Under these circumstances we observe that the above three schemes are valid for $j = 2(1)J$ and for $n = 0(1)N$.

We are asked to perform two experiments one in which the width of the Gaussian bell specified in (34) is wide for which $\sigma = \frac{1}{10}L_x$, and one in which it is narrow for which $\sigma = \frac{1}{1000}L_x$. The latter experiment is constructed to display the peculiarities of the schemes in the presence of fronts, that is, large gradients.

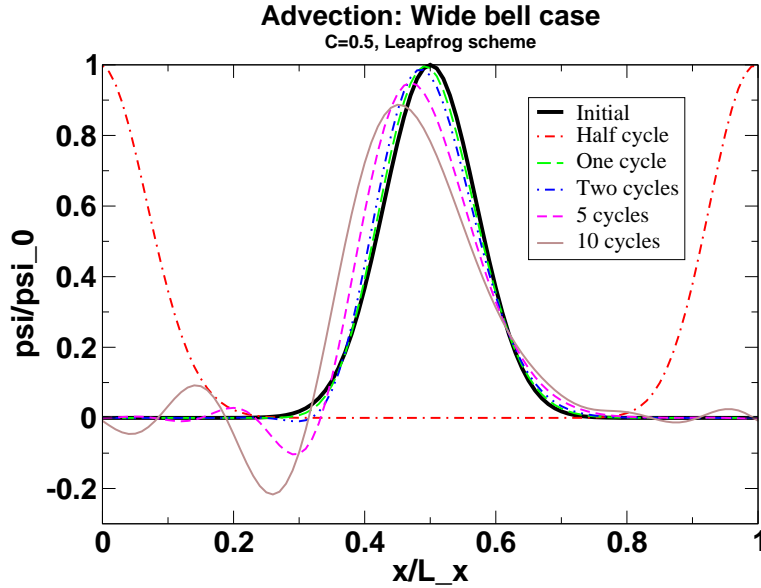


Figure 4: This is the solution for the initial wide bell function using the leapfrog scheme with $C = 0.5$.

f.

Show that the numerical analogue of (35) is

$$\psi_{j+j}^n = \psi_j^n \quad \text{for } j = 1(1)\cdots, \quad (37)$$

and the numerical analogue of the initial condition is

$$\psi_j^0 = \psi_0 e^{-\left(\frac{x_j - x_0}{\sigma}\right)^2} \quad \text{for } j = 1(1)J + 1. \quad (38)$$

g.

Solve (31) using the leapfrog, upwind/upstream and Lax-Wendroff schemes subject to the conditions (37) and (38). Stop the computations after 10 cycles, that is, when the peak of the bell has traversed ten times the distance L_x . Do one experiment with the Courant number $C = 0.5$ and another with $C = 1$. Please also feel free to experiment with other Courant numbers $\frac{1}{2} < C < 1$. Plot the solution after 1/2, 1, 2, 5 and 10 cycles together with the initial tracer distribution for each of the two Courant number values. Lump the plots for the concentration as a function of distance into one plot for each scheme, that is, six curves on each plot, as exemplified in Figure 4.

h.

Discuss the solutions based on the plots. What characterizes the solution as it evolves in time? Which of the solutions are diffusive and which are dispersive? What are the characteristics of these processes?

i.

Finally we consider the simplified advection-diffusion equation

$$\partial_t \psi + A \partial_x \psi = \kappa \partial_x^2 \psi. \quad (39)$$

where the advection speed A as well as the mixing coefficient κ is constant. Construct a scheme that is stable and consistent for (39) and state the stability condition. Explain your choices.

6 Problem set: Geostrophic Adjustment

One of the most important and strongest balances in the atmosphere and ocean, confirmed over and over again by observations, is geostrophy. When the fluid motion is in geostrophic balance we have a balance between the Coriolis acceleration and the pressure forcing, that is,

$$f\mathbf{k} \times \mathbf{u}_g = -\frac{1}{\rho_0}\nabla_H p, \quad \text{or} \quad v_g = \frac{1}{\rho_0 f}\partial_x p, \quad u_g = -\frac{1}{\rho_0 f}\partial_y p, \quad (40)$$

where $f = 2\Omega \sin \phi$ is the Coriolis parameter, \mathbf{k} is the unit vector along the vertical z -axis, \mathbf{u}_g is the (horizontal) geostrophic velocity with components u_g, v_g along the x -axis and y -axis, respectively, ρ_0 is the density, $\nabla_H = \mathbf{i}\partial_x + \mathbf{j}\partial_y$ is the horizontal component of the three-dimensional del-operator, and p is pressure. Note that (40) contains three unknowns, namely $p, u_g,$ and $v_g,$ but only two equations. Hence the solution is undetermined. Only by specifying one of them, say the pressure $p,$ can we find the two other variables.

A fundamental question is therefore how the atmosphere and ocean actually adjust from an unbalanced state to one in geostrophic balance under gravity. This problem, coined geostrophic adjustment (under gravity), was first raised by Carl Gustav Rossby³ back in the 1930s (*Rossby*, 1937, 1938), and is nicely summarized by *Blumen* (1972) and (*Gill*, 1982, Chapter 7, Section 7.2, page 191). It is the background for this computer problem. As usual we make the problem as simple as possible, but no simpler. Thus, we consider the one-dimensional (1-D) shallow water equations for this purpose. It conveniently serves the purpose of illustrating solution modes, the role of initial conditions and the use of an open boundary condition (FRS).

We recall that the shallow water equations assumes a hydrostatic balance and hence that $p = \rho_0 g h,$ where h is the geopotential height. Thus the governing equations, inherently non-linear, are

$$\partial_t h = -\nabla_H \cdot (h\mathbf{u}), \quad (41)$$

$$\partial_t \mathbf{u} = -f\mathbf{k} \times \mathbf{u} - \mathbf{u} \cdot \nabla_H \mathbf{u} - g\nabla_H h, \quad (42)$$

where the Coriolis parameter is $f = 1.26 \cdot 10^{-4} \text{s}^{-1}$ (corresponding to its value at 60°N). As is common we may regard h as the geopotential height of a pressure surface in the atmosphere and as the depth of a water column in the ocean. The equilibrium height of h in the atmosphere is associated with a pressure surface of $\approx 900 \text{hPa},$ while the equilibrium depth in the ocean is commonly $\approx 1 \text{km}.$

³Carl-Gustaf Arvid Rossby (1898 - 1957) was a Swedish-U.S. meteorologist who pioneered explaining the large-scale motions of the atmosphere in terms of fluid mechanics. Rossby came into meteorology and oceanography while studying under Vilhelm Bjerknes in Bergen in 1919, where Bjerknes' group was developing the concept of a polar front (the Bergen School of Meteorology). His name is associated with various quantities and phenomena in meteorology and oceanography, e.g., the Rossby number, Rossby's radius of deformation, and Rossby waves.

Part 1:**a.**

Show that by introducing $\mathbf{U} = h\mathbf{u}$ and $h = h$ as new variables then (41) and (42) become

$$\partial_t h = -\nabla_H \cdot \mathbf{U}, \quad (43)$$

$$\partial_t \mathbf{U} = -f\mathbf{k} \times \mathbf{U} - \nabla_H \cdot \left(\frac{\mathbf{U}\mathbf{U}}{h} \right) - \frac{1}{2}g\nabla_H h^2. \quad (44)$$

b.

Show that (41) and (42) may be combined to yield the vorticity equation

$$(\partial_t + \mathbf{u} \cdot \nabla_H)P_v = 0, \quad (45)$$

where P_v is the potential vorticity defined as

$$P_v = \frac{\zeta + f}{h}, \quad (46)$$

where in turn $\zeta = \mathbf{k} \cdot \nabla_H \times \mathbf{u}$ is the vorticity.

c.

Let us assume that the motion is independent of y ($\partial_y = 0$). Show that under these circumstances (41) and (42) reduces to

$$\partial_t h = -u\partial_x h - h\partial_x u, \quad (47)$$

$$\partial_t u = fv - u\partial_x u - g\partial_x h, \quad (48)$$

$$\partial_t v = -fu - u\partial_x v, \quad (49)$$

and show that the steady state solution to (47) - (49) then is one in geostrophic balance and given by

$$u = 0 \quad \text{and} \quad v = \frac{g}{f}\partial_x h. \quad (50)$$

d.

Utilize (45) and (50) to show that the steady state solution to (47) - (49) is a solution to the ordinary differential equation

$$\partial_x^2 h - \frac{fP_{v0}}{g}h = -\frac{f^2}{g}, \quad (51)$$

where $P_{v0} = P_{v0}(x)$ is the initial distribution of the potential vorticity.

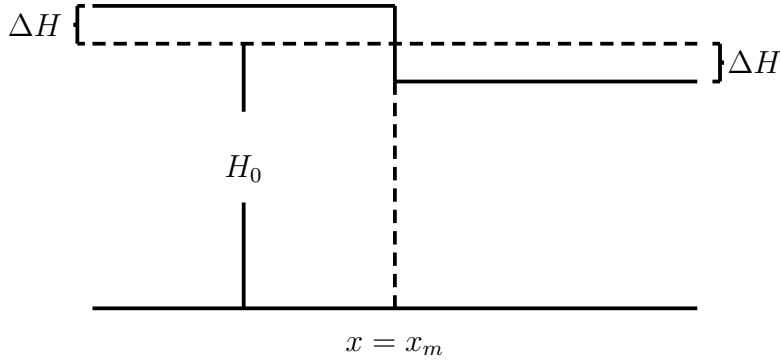


Figure 5: Depicted is the initial geopotential height according to (52).

e.

Let us assume that the initial condition is one at rest, and that the geopotential height is given by a Heaviside function, that is,

$$u = v = 0, \quad \text{and} \quad h(x, t) = H_0 - \text{sgn}(x - x_m)\Delta H \quad (52)$$

where $\text{sgn}(\psi) = +1$ if $\psi \geq 0$ and $\text{sgn}(\psi) = -1$ if $\psi < 0$ (Figure 5). Show that under these circumstances the solution to (51) is

$$h = H_0 + \Delta H \begin{cases} 1 - \frac{2\lambda_-}{\lambda_- + \lambda_+} e^{\frac{x-x_m}{\lambda_-}} & \text{if } x < x_m \\ -1 + \frac{2\lambda_+}{\lambda_- + \lambda_+} e^{-\frac{x-x_m}{\lambda_+}} & \text{if } x \geq x_m \end{cases} . \quad (53)$$

where $\lambda_{\pm} = \frac{1}{f} \sqrt{g(H_0 \mp \Delta H)}$ is the Rossby radii of deformation, and where $H_0 = 1000$ m, $\Delta H = 15$ m, $u_g = 0$ ms⁻¹, and $x_m = D/2$ is the middle point of the domain of length D . Is the $h - H_0$ negative or positive at $x = x_m$? Discuss the solution.

f.

If you were to solve the system (47) - (49), how many boundary and initial conditions do you have at your disposal? Explain how you derived the number of conditions.

Part 2:

We will solve the system (47) - (49) using numerical methods for a limited domain $x \in \langle 0, D \rangle$. To this end we need boundary conditions at $x = 0, D$ and initial conditions at time $t = 0$. We assume that the motion is started from one at rest and where the geopotential height (or ocean surface) is given by (52).

g.

To solve (47) - (49) you may either use the leapfrog scheme or the method of characteristics. Describe in some detail how you derive the finite difference approximation to the various terms. Explain your choices. Hint: If you choose to use leapfrog use a filter to remove the two gridlength noise (cf. the Lecture Notes).

h.

Is the scheme consistent? Derive under what condition(s) the scheme is stable? Describe in some detail how you analyzed the stability and consistency of the scheme⁴. How long time step Δt can be used? Explain your choice.

i.

Solve the above equations numerically using the scheme you have chosen and constructed for the domain $x \in \langle 0, D \rangle$. Assume that the variables u , v , and h retain their initial values at the boundaries $x = 0$ and $x = D$. Further, let the grid length be $\Delta x = 100\text{km}$ and $D = 62\Delta x$.

Plot h after 1.5, 3.0, 4.5, 6 and 10 hours into the future. Discuss the solution. Try to make a movie spanning $t \in [0, 10]\text{hrs}$. What kind of waves do you observe?

j.

Repeat the above computation using the the FRS method to relax the inner solution towards the externally specified values $(\hat{u}, \hat{v}, \hat{h}) = (0, 0, H_0 + \Delta H)$ at $x = 0$ and $(\hat{u}, \hat{v}, \hat{h}) = (0, 0, H_0 - \Delta H)$ at $x = D$. Let the buffer zone be seven points wide where the relaxation parameter λ_j is as given in Table 1.

j	λ_j	j
1	1.0	j_{max}
2	0.69	$j_{max} - 1$
3	0.44	$j_{max} - 2$
4	0.25	$j_{max} - 3$
5	0.11	$j_{max} - 4$
6	0.03	$j_{max} - 5$
7	0.0	$j_{max} - 6$

Table 1: Values of the relaxation parameter used in Part 2, item **j**. The left-hand column refers to the j numbers in the left-hand FRS zone, where $x = 0$ corresponds to $j = 1$. The right-hand column refers to the right-hand FRS zone where $x = D$ corresponds to $j = j_{max}$.

⁴Hint: Neglect the non-linear terms when performing the stability analysis.

Compare the solution to the steady state solution you derived in item **e**, for instance by plotting the difference between them. Explain and discuss any differences you observe.

k.

Compute the geostrophic component of the velocity

$$v_g = \frac{g}{f} \partial_x h \quad (54)$$

using the solution for h at $t = 6$ hours. Compare v_g and v at $t = 6$ hours and describe and discuss what you observe. What do you think have happened?

l.

Finally, replace the initial condition for v in (53) by

$$v = \frac{g}{f} \partial_x h_s. \quad (55)$$

where h_s is the steady state solution (52). Discuss the solution.

7 Problem set: Flux correction methods

We continue to consider numerical solutions to the advection equation (31) in which the advection speed is not necessarily a constant. Writing the advection equation in flux form we get

$$\partial_t \theta + \partial_x(u\theta) = 0 \quad (56)$$

where θ is the tracer concentration.

Part 1:

a.

Show that

$$\theta_j^{n+1} = \theta_j^n - (F_j^n - F_{j-1}^n), \quad (57)$$

is a first order finite difference approximation (in a non-staggered grid) to (56) where

$$F_j^n = \frac{1}{2} [(u_j^n + |u_j^n|) \theta_j^n + (u_{j+1}^n - |u_{j+1}^n|) \theta_{j+1}^n] \frac{\Delta t}{\Delta x}. \quad (58)$$

b.

Show that the scheme in (57) has a truncation error of order Δt og Δx .

c.

Show that the scheme in (57) is a second approximation to the advection-diffusion equation

$$\partial_t \theta + \partial_x(u\theta) = \kappa \partial_x^2 \theta \quad \text{hvor} \quad \kappa = \frac{1}{2} |u| (\Delta x - |u| \Delta t), \quad (59)$$

assuming that the velocity is a slowly varying function in time and space.

d.

Equation (59) tells us that (57) has an inherent diffusion with a diffusion coefficient given by κ . Visualize this by solving (57) numerically for $x \in \langle 0, L \rangle$ where $L = 2000\text{km}$. Let the space increment be $\Delta x = 20\text{km}$, and the velocity be constant, say $u = u_{\max} = 1\text{m/s}$, and $t_n = n\Delta t$ where n is the time counter and Δt is the time step. As in Computer Problem #3 on page 12 we make use of cyclic boundary conditions at $x = 0$ and $x = L$. The initial condition is

$$\theta|_{t=0} = \theta_0 e^{-\left(\frac{2x-L}{4\Delta x}\right)^2} \quad (60)$$

where the tracer amplitude is $\theta_0 = 1$.

Plot the results after 1, 3, 5 and 10 days together with the initial tracer concentration. To this end you need to specify the time step. Explain and discuss your choice.

Describe and discuss what you observe by comparing the evolution of the tracer concentration with the initial tracer distribution. Explain what have happened.

Part 2:

According to *Smolarkiewicz* (1983) it is possible to counteract the inherent numerical diffusion in the upwind scheme by adding a correction term, or an advective flux u^*C , to (56). The velocity u^* is the so called *antidiffusive velocity*, and is defined by

$$u^* = \kappa \begin{cases} \partial_x \theta / \theta & , \quad \theta > 0 \\ 0 & , \quad \theta \leq 0 \end{cases} . \quad (61)$$

that is solving the equation

$$\partial_t \theta + \partial_x [(u + u^*)\theta] = 0. \quad (62)$$

rather than (56).

e.

Solve (62) using the MPDATA method, that is, the predictor-corrector method. Use first the iterative method with at least two steps, then the simple method of scaling the antidiffusive velocity. Let the parameters and initial condition be as in Part 1, item **d.** When scaling use a scaling factor of $S_c = 1.3$. When computing the antidiffusive velocity use a centered in space finite difference approximation, and ensure that you add, as suggested by *Smolarkiewicz* (1983), a small number $\epsilon = 10^{-15}$ in the denominator.

f.

Why do we have to add the small number ϵ to the denominator?

g.

Make experiments varying the scaling factor S_c . Try out other finite difference approximations to the antidiffusive velocity. Discuss the results.

8 Problem set: Planetary waves

One of the most important and strongest balances in the atmosphere and ocean, confirmed over and over again by observations, is geostrophy. When the fluid motion is in geostrophic balance we have a balance between the Coriolis acceleration and the pressure forcing, that is,

$$f\mathbf{k} \times \mathbf{u}_g = -\frac{1}{\rho_0}\nabla_H p, \quad \text{or} \quad v_g = \frac{1}{\rho_0 f}\partial_x p, \quad u_g = -\frac{1}{\rho_0 f}\partial_y p, \quad (63)$$

where $f = 2\Omega \sin \phi$ is the Coriolis parameter, \mathbf{k} is the unit vector along the vertical z -axis, \mathbf{u}_g is the (horizontal) geostrophic velocity with components u_g, v_g along the x -axis and y -axis, respectively, ρ_0 is the density, $\nabla_H = \mathbf{i}\partial_x + \mathbf{j}\partial_y$ is the horizontal component of the three-dimensional del-operator, and p is pressure. Note that (63) contains three unknowns, namely $p, u_g,$ and $v_g,$ but only two equations. Hence the system is undetermined. Only by specifying one of them, say the pressure $p,$ can we find the two other variables.

A fundamental question is therefore how the atmosphere and ocean actually adjust from an unbalanced state to one in geostrophic balance under gravity. This problem, coined geostrophic adjustment (under gravity), was first raised by Carl Gustav Rossby⁵ back in the 1930s (*Rossby*, 1937, 1938), and is the background for this computer problem. As usual we make the problem as simple as possible, but no simpler. Thus, we consider the one-dimensional (1-D) shallow water equations for this purpose. It also conveniently serves the purpose of illustrating solution modes, the role of initial conditions and the use of an open boundary condition (FRS).

We recall that the shallow water equations assumes a hydrostatic balance and hence that $p = \rho_0 g h,$ where h is the geopotential height. Thus the governing equations, inherently non-linear, are

$$\partial_t h = -\nabla_H \cdot (h\mathbf{u}), \quad (64)$$

$$\partial_t \mathbf{u} = -f\mathbf{k} \times \mathbf{u} - \mathbf{u} \cdot \nabla_H \mathbf{u} - g\nabla_H h, \quad (65)$$

where the Coriolis parameter is $f = 1.26 \cdot 10^{-4} \text{s}^{-1}$ (corresponding to its value at 60°N). As is common we may regard h as the geopotential height of a pressure surface in the atmosphere and as the depth of a water column in the ocean. The equilibrium height of h in the atmosphere is associated with a pressure surface of $\approx 900\text{hPa},$ while the equilibrium depth in the ocean is commonly $\approx 1\text{km}.$

⁵Carl-Gustaf Arvid Rossby (1898 - 1957) was a Swedish-U.S. meteorologist who pioneered explaining the large-scale motions of the atmosphere in terms of fluid mechanics. Rossby came into meteorology and oceanography while studying under Vilhelm Bjerknes in Bergen in 1919, where Bjerknes' group was developing the concept of a polar front (the Bergen School of Meteorology). His name is associated with various quantities and phenomena in meteorology and oceanography, e.g., the Rossby number, Rossby's radius of deformation, and Rossby waves.

Part 1:**a.**

Show that by introducing $\mathbf{U} = h\mathbf{u}$ and $h = h$ as new variables (64) and (65) become

$$\partial_t h = -\nabla_H \cdot \mathbf{U}, \quad (66)$$

$$\partial_t \mathbf{U} = -f\mathbf{k} \times \mathbf{U} - \nabla_H \cdot \left(\frac{\mathbf{U}\mathbf{U}}{h} \right) - \frac{1}{2}g\nabla_H h^2. \quad (67)$$

b.

Show that by letting $\mathbf{u}'(x, t)$ and $h'(x, t)$ denote the deviations away from a background state in geostrophic balance, that is,

$$\mathbf{u} = u_g \mathbf{i} + \mathbf{u}'(x, t), \quad h = H(y) + h'(x, t), \quad \text{where} \quad u_g = -\frac{g}{f} \partial_y H \quad (68)$$

then (64) and (65) reduces to

$$\partial_t h = -u \partial_x h - h \partial_x u, \quad (69)$$

$$\partial_t u = f v - u \partial_x u - g \partial_x h, \quad (70)$$

$$\partial_t v = -f(u - u_g) - u \partial_x v, \quad (71)$$

where primes on u , v and h are dropped for clarity.

c.

If you were to solve the system (69) - (71), how many boundary and initial conditions do you have at your disposal? Explain how you derived the number of conditions.

Part 2:

We will solve the system (69) - (71) using numerical methods for a limited domain $x \in \langle 0, D \rangle$. To this end we need boundary conditions at $x = 0, D$ and initial conditions at time $t = 0$. We assume that the motion is started from one at rest in which the geopotential height (or ocean surface) is perturbed. Thus the initial conditions are

$$u = v = 0, \quad \text{and} \quad h(x, t) = H_0 + A e^{-\left(\frac{x-x_m}{\sigma}\right)^2} \quad (72)$$

where $H_0 = 1000$ m, $A = 15$ m, $u_g = 0$ ms⁻¹, $x_m = D/2$ is the middle point of the domain, and σ is a measure of the width of the Gaussian bell.

d.

To solve (69) - (71) we will adopt the leapfrog scheme. Construct the scheme so that

$$\frac{h_j^{n+1} - h_j^{n-1}}{2\Delta t} = -DIVH, \quad (73)$$

$$\frac{u_j^{n+1} - u_j^{n-1}}{2\Delta t} = CORU + ADVU + PRES, \quad (74)$$

$$\frac{v_j^{n+1} - v_j^{n-1}}{2\Delta t} = CORV + ADVV \quad (75)$$

where Δt is the time step, $DIVH$ is the divergence term in (69), $CORU$, $CORV$ are the respective Coriolis terms and $ADVU$, $ADVV$ the respective advection terms in (70) and (71), and $PRES$ is the pressure term in (70).

Describe in some detail how you derive the finite difference approximation to the various terms. Explain why you make the choices you make.

e.

Is the scheme stable and consistent? If so, why and under what condition(s) is the scheme stable? Describe in some detail how you analyzed the stability and consistency of the scheme⁶. How long time step Δt can be used? Explain your choice.

f.

Solve the above equations using the scheme (73) - (75) you have constructed for the domain $x \in \langle 0, D \rangle$. Assume that the variables u , v , and h retain their initial values at the boundaries $x = 0$ and $x = D$. Further, let the grid length be $\Delta x = 100\text{km}$, $D = 62\Delta x$ and $\sigma = 5\Delta x$.

Plot h after 1.5, 3.0, 4.5, 6 and 10 hours into the future. Discuss the solution. Try to make a movie spanning $t \in [0, 10]\text{hrs}$. What kind of waves do you observe?

g.

Repeat the above computation using the the FRS method to relax the inner solution towards the externally specified values $(\hat{u}, \hat{v}, \hat{h}) = (0, 0, H_0)$ in a buffer zone seven points wide where the relaxation parameter λ_j is given in Table 2 on page 26.

Compare the solution to the one you obtained performing the computation in item **f**, for instance by plotting the difference between them. Explain and discuss any differences you observe.

⁶Hint: Neglect the non-linear terms when performing the stability analysis.

j	λ_j	j
1	1.0	j_{max}
2	0.69	$j_{max} - 1$
3	0.44	$j_{max} - 2$
4	0.25	$j_{max} - 3$
5	0.11	$j_{max} - 4$
6	0.03	$j_{max} - 5$
7	0.0	$j_{max} - 6$

Table 2: Values of the relaxation parameter used in Part 2, item g.

h.

Compute the geostrophic component of the velocity

$$v_g = \frac{g}{f} \partial_x h \quad (76)$$

using the solution for h at $t = 6$ hours. Compare v_g and v at $t = 6$ hours and describe and discuss what you observe. What do you think have happened?

i.Finally, replace the initial condition for v in (72) by

$$v = \frac{g}{f} \partial_x h. \quad (77)$$

and repeat item g.. Discuss the solution by comparing it to the solution obtained through item g. above.

9 Problem set: Rossby waves

The response of the atmosphere an ocean consists in many cases of various types of waves. One important distinct type of wave response is the barotropic Rossby wave *LaCasce* (2009). These waves are unique in the sense that their phase velocity is westward while their group velocity is eastward. Since the energy of the waves propagates with the group velocity it implies that the waves tend to die out as they propagate westward. Another unique feature is that the phase velocity or wave speed depends on the rate at which the Earth's rotation changes with latitude. Hence the wave speed decreases with latitude. Consequently the Rossby waves are hard to observe at high latitudes.

The equation governing these waves is derived from the linear, barotropic shallow water equation, that is,

$$\partial_t \mathbf{u} + f \mathbf{k} \times \mathbf{u} = -\nabla_H \phi, \quad (78)$$

$$\partial_t \phi + c_0^2 \nabla_H \cdot \mathbf{u} = 0, \quad (79)$$

with the additional assumption that the motion is effectively divergence free. Thus we get

$$\partial_t \zeta + \beta \partial_x \psi = 0, \quad (80)$$

where ψ is the streamfunction, that is, $\mathbf{u} = \mathbf{k} \times \nabla_H \psi$ and $\zeta = \mathbf{k} \cdot \nabla_H \times \mathbf{u}$ is the vorticity. The constant $\beta = 2 \cdot 10^{-11} (ms)^{-1}$ represents the first order effect of the impact of the change in the Earth's rotation rate with latitude, that is, the first derivative in a Taylor series expansion of the Coriolis parameter f with respect to the latitude y , viz.,

$$f(y) = f|_{y=y_0} + \beta(y - y_0) + O([y - y_0]^2) \quad \text{where} \quad \beta = \partial_y f|_{y=y_0}. \quad (81)$$

Here we will solve the one-dimensional version of (80) by numerical means. Thus the governing equation we will solve is

$$\partial_t (\partial_x^2 \psi) + \beta \partial_x \psi = 0. \quad (82)$$

Part 1: Analysis

a.

Show that (82) follows from (78) and (79) and discuss under the assumption under which it is correct. For instance, what physics are neglected?

b.

Show that the wave solution

$$\psi(x, t) = \text{Re} \{ A e^{i\alpha(x-ct)} \} \quad (83)$$

is a is solution to (82), where c is the phase speed and α is the wavenumber. Note that A is an imaginary number so that the solution may be written

$$\psi = A_r \cos \alpha(x - ct) - A_i \sin \alpha(x - ct), \quad (84)$$

where $A_r = \text{Re} \{A\}$ is the real part of A and $A_i = \text{Im} \{A\}$ is the imaginary part of A .

c.

Show that the phase speed c of the Rossby wave is

$$c = -\frac{\beta}{\alpha^2}. \quad (85)$$

and that the group velocity, c_g is

$$c_g = -c. \quad (86)$$

d.

How many boundary/initial conditions must be specified in order to solve (82)?

e.

Before we solve (82) numerically within the finite domain $x \in \langle 0, L \rangle$ we make it non-dimensional. Show that by choosing a typical time scale given by

$$T = \frac{1}{\beta L}, \quad (87)$$

the non-dimensional version of (82) becomes

$$\partial_t^* (\partial_{x^*}^2 \psi^*) + \partial_{x^*}^* \psi^* = 0, \quad ; \quad \forall x^* \in \langle 0, 1 \rangle, \quad (88)$$

or

$$\partial_t (\partial_x^2 \psi) + \partial_x \psi = 0, \quad ; \quad \forall x \in \langle 0, 1 \rangle, \quad (89)$$

where we have dropped the stars for clarity.

Part 2: Numerical solutions

We will experiment with three different initial distributions for the streamfunction, namely a simple wave, a more complex wave and a Gaussian distribution, that is,

$$\psi|_{t=0} = \begin{cases} \sin \alpha x & \text{the simple wave} \\ \sin \alpha x \cos \alpha x & \text{more complex wave} \\ e^{-\left(\frac{x-x_0}{\sigma}\right)^2} & \text{Gaussian distribution} \end{cases} \quad (90)$$

where α is a finite non-dimensional wavenumber different from zero, $x_0 = 0.5$ is the half-distance of the computational domain, and $\sigma = 0.001$ is a measure of the (narrow) width of the Gaussian bell. Let $\alpha = m\pi$, $m = 5$ for the simple and more complex wave. We note that the latter makes $\psi = 0$ at $x = 0, 1$ at time $t = 0$.

To solve (89) we first split it in two, that is,

$$\partial_t \zeta + \partial_x \psi = 0, \quad (91)$$

and

$$\partial_x^2 \psi = \zeta, \quad (92)$$

where ζ is the non-dimensional vorticity. Thus we first find the vorticity by solving the time marching equation (91), and then the streamfunction by solving the Helmholtz equation (92). To solve (91) and (92) numerically properly we must choose a space increment Δx small enough to resolve the dominant waves given in (90). Next the time increment Δt must be chosen so that the stability condition is satisfied, if any.

d.

Show that the non-dimensional wave speed is

$$c = -\frac{1}{\alpha^2}. \quad (93)$$

e.

Construct a CTCS scheme for (91) and (92) that results in an explicit, consistent, neutral and conditionally stable scheme, and derive the condition for stability.

f.

Solve (91) and (92) within the domain $x \in \langle 0, 1 \rangle$ using the CTCS scheme constructed under subsection **e.** using the three initial conditions (90) and appropriate boundary condition to mimic an infinite plane. Show that the latter is satisfied by making use of the periodic boundary condition

$$\psi(x, t) = \psi(x + 1, t). \quad (94)$$

and the fact that

$$\partial_t \psi + c \partial_x \psi = 0 \quad \text{at} \quad x = 0, \quad (95)$$

where c is the non-dimensional wave speed given in (93).

g.

Plot the solution in a Hovmöller diagram in the x, t space with x along the horizontal axis and t along the vertical axis. Verify your numerical solution by reading off the wave speed from the Hovmöller diagram and check it against the true wave speed given in (93).

h.

Solve (91) and (92) using the CTCS scheme but this time within a closed domain. Show first that a closed domain requires that

$$\psi = 0 \quad \text{at} \quad x = 0, 1. \quad (96)$$

Next plot the solution as a function of x for different times, and also in a Hovmöller diagram as in item **g**. Note that the solution in this case becomes an oscillation.

10 Problem set: Storm surges

We consider below the storm surge problem. The purpose is to gain experience in constructing numerical solutions to geophysical problems that include more than one dependent variable.

The water level of the ocean changes due to three main factors. For one it responds to the astronomical forcing which gives rise to the well known tidal phenomenon, a deterministic periodic response in the water level. Next the water level in the ocean changes due to the forcing exerted by the atmosphere through wind stress and sea level pressure. This phenomenon is referred to as the storm surge response and its associated water level change is referred to as the storm surge. From time to time the joint occurrence of high tides and high storm surges can lead to devastating high water levels even along the Norwegian coast. One such example is from mid October 1987 where the water level in Oslo Harbour reached 1.96 meters above normal sea level. More examples are given in *Gjevik* (2009). Finally the water level of the ocean may change due to expansion by heating. This latter is a concern with regard to climate change in that the water level rises under global warming.

To secure life and property many countries early on developed forecasts services for tides and storm surges. As numerical ocean models were developed in the late 1960s and early 1970s one of the first models that were developed was in fact numerical models to forecast storm surges and tides. For instance the Proudman Ocean Laboratory in Liverpool, UK (now merged within NOC - the National Oceanography Center) was founded in the late 1960s to forecast tides and storm surges in British waters, and has since then been one of the leading institutions within this field. Since the late 1970s and early 1980s also the Norwegian Meteorological Institute has developed numerical models to forecast sea level changes due to storm surges and tides using numerical models developed through the work of *Gjevik and Røed* (1976), *Martinsen et al.* (1979) and *Røed* (1979).

Many of the earlier studies of storm surges, including those just referenced, have shown that the storm surge is mainly a barotropic response. To construct a storm surge model we may therefore use an ocean in which we assume the density to be constant in time and space. The equations therefore reduce to the well known shallow water equations. Let

$$\mathbf{U}(x, y, t) = \int_{-H(x,y)}^{\zeta(x,y,t)} \mathbf{u}(x, y, z, t) dz, \quad (97)$$

with components (U, V) along the x, y -axes, respectively, be the transport of water in a water column of depth $h = H + \zeta$ where ζ is the sea level deviation away from the equilibrium depth H (see Figure 6). Then the shallow water equations are

$$\begin{aligned} \partial_t \mathbf{U} + \nabla_H \cdot (h^{-1} \mathbf{U} \mathbf{U}) + f \mathbf{k} \times \mathbf{U} &= -gh \nabla_H (h - H) + \rho_0^{-1} (\boldsymbol{\tau}_s - \boldsymbol{\tau}_b), \\ \partial_t h + \nabla_H \cdot \mathbf{U} &= 0. \end{aligned} \quad (98)$$

where $\boldsymbol{\tau}_s$ and $\boldsymbol{\tau}_b$ are respectively the wind and bottom stresses with components (τ_s^x, τ_s^y) og (τ_b^x, τ_b^y) , g is the gravitational acceleration and ρ_0 is the (uniform in time and space) density. The Coriolis parameter is $f = 2\Omega \sin \phi$ where Ω is the Earth's rotation rate and ϕ is the latitude.

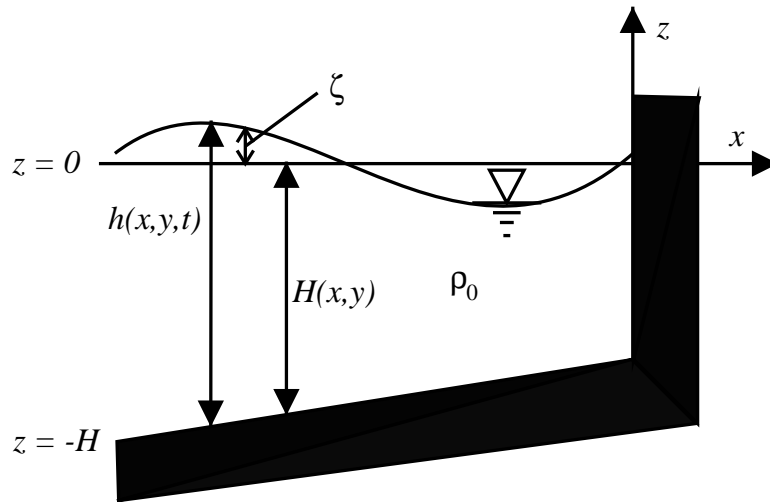


Figure 6: Sketch of a storm surge model along a straight coast conveniently showing some of the notation used.

We observe that the second term on the left-hand side and the first term on right-hand side of (98) are non-linear terms. The main effect of these terms is to get the interaction of tides and storm surges correct. In many instances this effect is small, and in the remainder we will neglect them. To make things a bit simpler we will also look for solution of the storm surge problem in the presence of a straight coast along the y -axis as sketched in Figure 6. Under these circumstances we may also neglect terms containing derivatives with respect to y , that is let $\partial_y = 0$. Thus by linearizing (98) and neglecting variations in the y direction we get

$$\begin{aligned}\partial_t U - fV &= -gH\partial_x h + \rho_0^{-1}(\tau_s^x - \tau_b^x), \\ \partial_t V + fU &= \rho_0^{-1}(\tau_s^y - \tau_b^y), \\ \partial_t h + \partial_x U &= 0.\end{aligned}\tag{99}$$

It is also safe to neglect the variation with latitude in the effect of the Earth's rotation. Thus we may safely assume that the Coriolis parameter is constant in time and space. In the following we will also assume that changes in the equilibrium depth are so small that H to a good approximation can be considered as being constant.

In summary we investigate linear, analytic and numerical solution to the storm surge problem along a straight coast on a flat bottom, that is, solutions to (99) in the domain $x \in [-\infty, 0]$ with constant depth. The initial condition is an ocean at rest and in equilibrium. Since the ocean is limited by the straight coast at $x = 0$ the natural boundary condition there is no flow through the coast. Since the other spatial boundary is at $x \rightarrow -\infty$ the domain is infinite. On the computer we have to limit it to a finite domain, that is, we have to stop the computations at a finite distance away from the coast, say $x = -L$. Then a boundary at $x \rightarrow -\infty$ is tantamount to saying that L is large compared to a typical dynamical length scale of the problem. The dominant length scale

in this problem, in fact for all shallow water problems, is the Rossby radius of deformation. Thus we have to let our choice of L be such that L is large compared to the Rossby radius. We note that the boundary at $x = -L$ is an open boundary. Thus the equations (99) are still valid there, and we have to construct a condition that does not violate them. If indeed L is large compared to the Rossby radius then we may safely assume that the dynamics are independent of x as well and the natural open boundary condition is therefore to let the solution approach the Ekman solution at $x = -L$.

Furthermore we let the parameters appearing in the governing equations be:

$$g = 10\text{ms}^{-1}, \quad \tau_s^x = 0\tau_s^y = 0.1\text{Pa}, \quad \rho_0 = 10^3\text{kg/m}^3, \quad f = 10^{-4}\text{s}^{-1},$$

$$H = 300\text{m}, \quad \tau_b^x = \rho_0 R \frac{U}{H}, \quad \tau_b^y = \rho_0 R \frac{V}{H}, \quad R = 2.4 \cdot 10^{-3}\text{m/s}. \quad (100)$$

if not explicitly deviated.

Part 1:

We first look for analytic solution to (99). Even the simple system (99) is too complex. Although the analytic solution constitutes an approximation to the problem, it can nevertheless be used to verify that the numerical solution is well behaved.

a.

Show that (99) follows by linearizing (98) under the assumption that changes in the equilibrium depth H are insignificant and that $|\mathbf{U}|^2 \ll |\mathbf{U}|$.

b.

Explain why the Ekman solution (101) is the natural open boundary condition to use at $x = -L$, and show that it may be written in the form

$$h = H \quad \text{or} \quad \partial_x h = 0 \quad \text{at} \quad x = -L, \quad \forall t. \quad (101)$$

Show also that the boundary condition at $x = 0$ is

$$U = 0 \quad \text{at} \quad x = 0 \quad \forall t. \quad (102)$$

and that the initial condition may be formulated as

$$U = V = 0, \quad \zeta = 0 \quad \text{at} \quad t = 0 \quad \forall x. \quad (103)$$

c.

Show that the inertial oscillations, that is, solutions that oscillates with the inertia frequency f , are avoided if we neglect the term $\partial_t U$ in (99).

d.

Show that under the assumption that $\partial_t U$ is small compared to the Coriolis acceleration the motion along the coast (in the y -direction) is in geostrophic balance. Furthermore, show that the analytic solution to (99), under this assumption and under the assumption that there is no bottom stress ($R = 0$), is

$$U = U_E \left(1 - e^{-\frac{x}{L_R}}\right) \quad (104)$$

$$V = ftU_E e^{-\frac{x}{L_R}} \quad (105)$$

$$h = H \left(1 + \frac{tU_E}{L_R H} e^{-\frac{x}{L_R}}\right) \quad (106)$$

where $L_R = \sqrt{gH}/f$ is Rossby's radius of deformation and

$$U_E = \frac{\tau_s^y}{\rho_0 f}, \quad (107)$$

is the Ekman transport, that is, the transport you get when solving the steady state version ($\partial_t = 0$) of (99) with $\partial_x = 0$ og $R = 0$.

e.

Solve (99) analytically under the assumption that $\tau_b^x = 0, \tau_b^y = \rho_0 Rv$, and that the term $\partial_t U$ in (99) can be neglected⁷.

f.

Plot the analytical solutions of h, U and V derived under **d.** and **e.** in a $x - t$ diagram, sometimes referred to as a Hovmöller diagram.

g.

What changes are introduced to (99) if the changes in the equilibrium depth H are significant?

Part 2:

In this part we investigate numerical solutions to (99) and the assumption that the depth is constant. Furthermore we let the parameters be given by (100).

⁷Hint: Make use of Laplace transforms.

h.

Construct a centered in space and forward-backward in time scheme⁸ on a staggered B-grid. The B-grid is the one dimensional version of lattice B of *Mesinger and Arakawa (1976)* (page 47). Thus we assume that the U - and V -points are staggered one half grid length with respect to the h -points as sketched in Fig. 7.

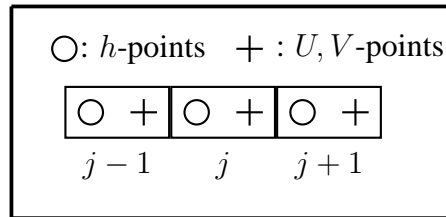


Figure 7: Displayed is the cell structure of lattice B of *Mesinger and Arakawa (1976)* in one space dimension. The circles are associated with h -points, while the horizontal bar is associated with U -points and the vertical bar with V -points within the same cells. The sketched staggering is such that the distance between adjacent h -points and U, V -points are one half grid distance apart.

i.

Show that your scheme constructed under item **h.** is neutrally stable under the condition

$$\Delta t \leq \frac{\Delta x}{c_0 \sqrt{1 + \left(\frac{\Delta x}{2L_R}\right)^2}} \quad (108)$$

using von Neumanns method⁹, and where $c_0 = \sqrt{gH}$. Discuss under which the simpler condition $C \leq 1$, where $C = c_0 \Delta t / \Delta x$ is valid. Is the scheme dissipative¹⁰?

j.

Show that your scheme constructed under item **h.** is consistent.

k.

Solve the storm surge problem (99) numerically making use of your scheme constructed under item **h.** and the parameters listed in (100) including the bottom stress. Choose Δx so that the (Rossby's) deformation radius, $L_R = c_0/f$, is well resolved, that is, $\Delta x \leq L_R/10$.

⁸Forward-backward in time means that as soon as one dependent variable is updated (in time) we use these values when updating the other dependent variables.

⁹Hint: When analysing the instability neglect all forcing (stress) terms.

¹⁰Hint: To analyze the dissipativeness analyse the growth factor.

i.

Plot the numerical solution of the dependent variables h , U og V in a Hovmöller diagram. Compare the numerical solution with those derived analytically under **d.** and **e.**. Discuss differences and similarities.

11 Problem set: Methods of characteristics applied to a non linear systems

We now solve the non-linear shallow water equations (98) on page 31 using the method of characteristics as outlined in the appendix of *Røed and O'Brien* (1983) (cf. Problem set: Storm surges on page 31). This problem is also associated with the semi-lagrangian method explained in Chapter 9 of *Røed* (2010).

a.

Show that if we define $c = \sqrt{gh}$ then (98) may be rewritten to yield the compatibility equations

$$\left(\frac{D^*}{dt}\right)_{1,2} (u \pm 2c) = fv + \frac{\tau_s^x - \tau_b^x}{\rho h} \quad (109)$$

$$\left(\frac{D^*}{dt}\right)_3 = -fu + \frac{\tau_s^y - \tau_b^y}{\rho h} \quad (110)$$

where the operators $\left(\frac{D^*}{dt}\right)_{1,2,3}$ are defined as

$$\left(\frac{D^*}{dt}\right)_{1,2,3} = \partial_t + \left(\frac{D^*x}{dt}\right)_{1,2,3} \partial_x \quad (111)$$

where

$$\left(\frac{D^*x}{dt}\right)_{1,2} = u \pm c, \quad \text{and} \quad \left(\frac{D^*x}{dt}\right)_3 = u, \quad (112)$$

are the characteristic equations.

b.

Solve (109) and (110) numerically using the method of characteristics with fixed space increments and time steps. Disregard the wind- and bottom stress and look for solutions for $t > 0$ assuming that the initial condition at $t = 0$ is given by

$$h|_{t=0} = H + \Delta H \tanh(\kappa x), \quad u|_{t=0} = v|_{t=0} = 0 \quad (113)$$

The solution domain is $x \in \langle -\frac{1}{2}L, \frac{1}{2}L \rangle$. Furthermore we let $\kappa = 10/L$, $\Delta H = H/2$, $H = 100\text{m}$ and $L = 2000\text{km}$. As boundary condition at $x = \pm\frac{1}{2}L$ we recommend to use the gradient condition or the "Flow Relaxation Scheme" (cf. the Lecture notes Chapter "Open boundary conditions").

c.

Display the solution in graphical form by plotting the time evolution of h , u , v , as isolines in the x, t space (Hovmøller diagram).

12 Problem set: Upwelling in the Bay of Guinea

In their pioneering work *Adamec and O'Brien* (1978) showed how an observed coastal upwelling event in the Bay of Guinea that was not forced by the local wind could be explained by wind events in the western equatorial Atlantic, and hence by events removed far away from the bay itself. The observed upwelling was puzzling because it could not be explained by local wind forcing, which was the prevailing explanation of coastal upwelling phenomena at the time.

Their starting point was that the Russian research vessel R/V *Passat*, that was located on the Equator about 10°W observed a significant and unexpected drop in the sea surface temperature (SST) *before* the seasonal upwelling in the Bay of Guinea was about to start. They also noted that the time difference between the two observations was just about right for an internal Kelvin wave to travel from the location of the research vessel to the Bay of Guinea¹¹. They therefore hypothesized that the observed upwelling event in the Bay of Guinea was remotely forced by an equatorially trapped, upwelling Kelvin wave generated by a pressure disturbance in the western part of the equatorial Atlantic. Once created it would travel eastward across the Atlantic basin towards the African coast, where it transforms into two coastal internal Kelvin waves, one propagating northward and a second propagating southward. The northward propagating one would then after some time hit the Bay of Guinea causing an upwelling event as the wave passed by. To support their hypothesis *Adamec and O'Brien* (1978) performed an experiment using a fairly simple, linear and numerical ocean model.

The objective is to reproduce the solutions of *Adamec and O'Brien* (1978). What they did was to simulate the equatorial Kelvin wave using a linear, reduced gravity model. Thus the governing equations we will solve are,

$$\partial_t \mathbf{u} + \beta y \mathbf{k} \times \mathbf{u} + g' \nabla_H h = \frac{\boldsymbol{\tau}}{\rho H} + A \nabla_H^2 \mathbf{u}, \quad (114)$$

$$\partial_t h + H \nabla_H \cdot \mathbf{u} = 0, \quad (115)$$

where $\nabla_H = \mathbf{i}\partial_x + \mathbf{j}\partial_y$, $\beta = 10^{-11}$ is the change of the Earth's rotation with latitude (the β -plane approximation), $g' = \Delta\rho/\rho$ is the reduced gravity where $\Delta\rho = 2\text{kg/m}^3$.

The computational domain they used is an idealized rendition of the Atlantic basin as sketched in Figure 8. The basin is 5000 km long and stretches 1500 km to the north and south of the equator. The presence of the African continent is in the form of a rectangular box 2000 km long and 1000 km wide protruding into the basin from the northeast corner of the basin.

To solve (114) and (115) we use an Arakawa C-grid of mesh size $\Delta x = \Delta y = 25\text{km}$ with the x -axis pointing eastward along the equator and the y -axis pointing northwards. Initially the ocean is at rest and in equilibrium with an upper layer equilibrium depth of $H = 50\text{m}$. The density difference between the upper and lower layer is $\Delta\rho = 2\text{kg/m}^3$. Use a time step of maximum 1/8 day. Furthermore let the eddy viscosity be $A = 10^2\text{m}^2/\text{s}$, and let the simulation span at least 120 days.

A motion is forced by applying a wind stress on the surface as displayed in Figure 9. The stress is pointing westward (from east towards west) so as to give upwelling at the equator.

¹¹This is actually the same mechanism that is the basis for the explanation of the El Niño phenomenon in the Pacific Ocean (*Hurlburt et al.*, 1976). Confer the website http://www.coaps.fsu.edu/lib/Florida_Consortium/enso_links.shtml for links to El Niño.

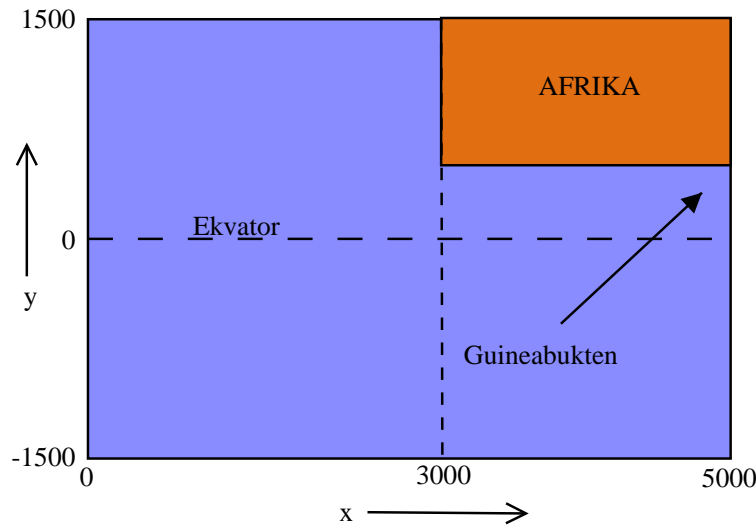


Figure 8: Sketch of the model domain for which (114) and (115) is to be solved.

Furthermore it is limited to act in the western part of the basin only. Thus the wind stress is,

$$\tau_s^x = -\tau_0 \begin{cases} 1 & ; 0 < x \leq a \\ \frac{b-x}{b-a} & ; a < x \leq b \end{cases}, \quad \tau_s^y = 0. \quad (116)$$

where $\tau_0 = 0.025$ Pa, $a = 1500$ km og $b = 2000$ km. We observe that there is no wind stress acting in the north-south direction, and that it does not change with latitude, but depend on the langitude such that it is zero east of $x = 2000$ km. In the finite difference approximation to (114) and (115) we use a CTCS¹² scheme (leapfrog). To avoid instabilities due to the diffusive term we employ the Dufort-Frankel approach for these terms. The diffusion terms allows us to specify a no-slip condition at the walls. Thus at the solid walls both velocity components are zero. To make $v = 0$ along the eastern (and western) boundary we make use of so called mirror points outside of the boundary as sketched in Figure 10. By letting the value of v in the mirrored point equals the value of v just inside the boundary, the linearly interpolated value at the boundary itself becomes zero as required. A similar approach is used at the northern and southern boundaries to make u equal zero there. We notice that the physical (real) boundaries goes through the points where the normal to the boundary velocity component are located. Thus the eastern and western boundaries goes through u -points, whil the northern and southern boundaries goes through v -points. With this configuration the coastlines fall exactly half way between the points where we compute the velocity component along the boundaries.

a.

Construct the finite difference approxiamtion (FDA) to (114) and (115) using the required scheme as alluded to above and write it down.

¹²CTCS - Centered in Time, Centered in Space.

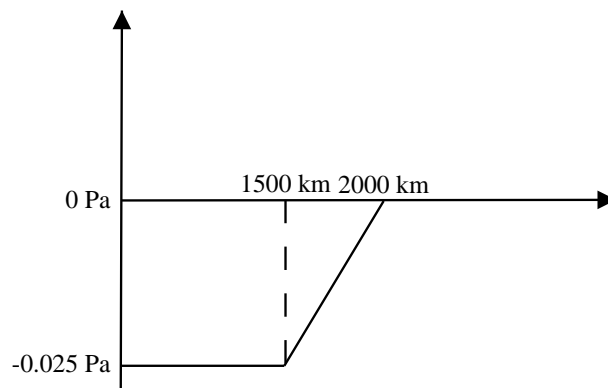


Figure 9: Skisse av vindstresset

b.

Why is it permissible to use the diffusive, dissipative and inconsistent Dufort-Frankel scheme for the FDA of the diffusion terms? What are the advantages? Explain how you would construct a scheme that is forward in time and centered in space and still stable.

c.

Construct a graph displaying contour lines of the thickness deviation $\Delta h = H - h$ after 10, 50 and 100 days and with a contour interval of 5m. Furthermore, construct a similar graph showing the velocities of the upper layer at day 50.

d.

Next construct a graph showing the thickness deviation in a Hovmöller diagram. Let the vertical axis be the time axis ranging from 0 to 120 days, and let the horizontal axis be 6000 km long. Let the first part run along the equator from $x = 2500$ km to $x = 5000$ km, the next 500 km along the eastern boundary north of the equator, the next 2000 km along the southern coast of Africa, and the last 1000 km along the north-eastern boundary (west Africa).

e.

Use the Hovmöller diagram to estimate the phase speed of the Kelvin wave and compare it to the analytic one entering the governing equations. Discuss the result.

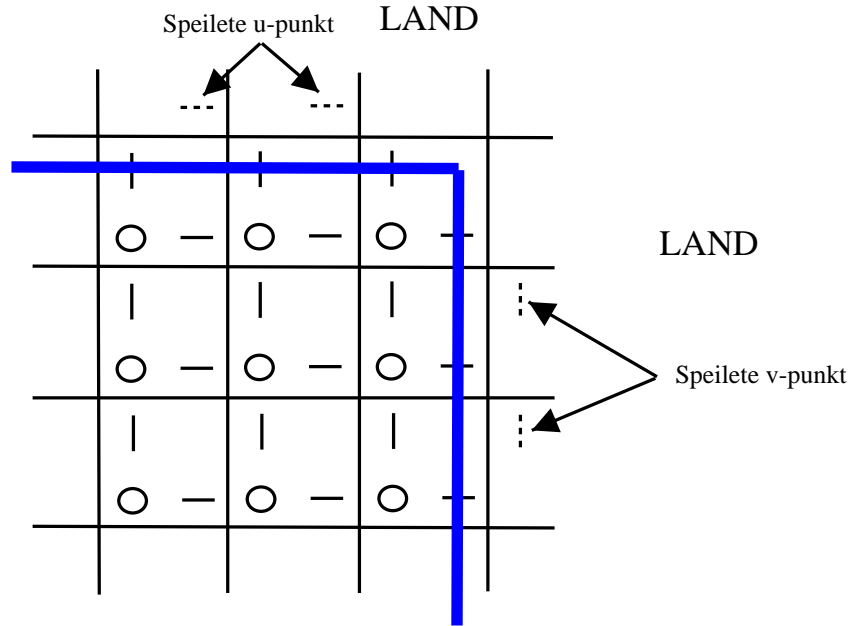


Figure 10: Spelling av hastighetspunketer ved faste render i et forskjøvet gitter. Sirkler, (O), angir h -punkter, horisontale streker, (-), u -punkter, mens vertikale streker, |, angir et v -punkt.

f.

Solve the non-linear version of (114) and (115), that is,

$$\partial_t \mathbf{u} + \mathbf{u} \cdot \nabla_H \mathbf{u} + \beta y \mathbf{k} \times \mathbf{u} + g' \nabla_H h = \frac{\tau}{\rho H} + A \nabla_H^2 \mathbf{u}, \quad (117)$$

$$\partial_t h + \nabla_H \cdot (h \mathbf{u}) = 0, \quad (118)$$

and plot the results in a similar manner as for the linear case. Discuss differences and similarities.

h.

Finally, construct an animation (movie) displaying the linear as well as the nonlinear results.

References

- Abramowitz, M., and I. Stegun, *Handbook of Mathematical Functions - ninth printing*, Dover Publications, Inc., 1965.
- Adamec, D., and J. J. O'Brien, The seasonal upwelling in the Gulf of Guinea due to remote forcing, *J. Phys. Oceanogr.*, 8, 1050–1060, 1978.
- Blumen, W., Geostrophic adjustment, *Rev. Geophys. Space Phys.*, 10, 485–528, 1972.

- Gill, A. E., *Atmosphere-ocean dynamics*, vol. 30 of *International Geophysical Ser.*, Academic Press, 1982.
- Gjevik, B., *Flo og fjære langs kysten av Norge og Svalbard*, Farleia Forlag, Norway, 2009, ISBN 978-82-998031-0-6.
- Gjevik, B., and L. P. Røed, Storm surges along the western coast of Norway, *Tellus*, 28, 166–182, 1976.
- Hurlburt, H. E., J. C. Kindle, and J. J. O'Brien, A numerical simulation of the onset of El Niño, *J. Phys. Oceanogr.*, 6, 621–631, 1976.
- LaCasce, J. H., *Atmosphere-ocean dynamics*, 2009, Class notes GEF4500, Dept. of Geosciences, University of Oslo, Norway.
- Martinsen, E. A., B. Gjevik, and L. P. Røed, A numerical model for long barotropic waves and storm surges along the western coast of Norway, *J. Phys. Oceanogr.*, 9, 1126–1138, 1979.
- Mesinger, F., and A. Arakawa, Numerical methods used in atmospheric models, GARP Publication Series No. 17, 64 p., World Meteorological Organization, Geneva, Switzerland, 1976.
- Røed, L. P., Storm surges in stratified seas, *Tellus*, 31, 330–339, 1979.
- Røed, L. P., *Fundamental of atmospheres and ocean on computers*, Lecture notes to GEF4510, Department of Geosciences, University of Oslo, P.O. Box 1022 Blindern, 0315 Oslo, Norway, 2010.
- Røed, L. P., and J. J. O'Brien, A coupled ice-ocean model of upwelling in the marginal ice zone, *J. Geophys. Res.*, 29, 2863–2872, 1983.
- Rossby, C. G., On the mutual adjustment of pressure and velocity distributions in certain simple current systems, *J. Mar. Res.*, 1, 15–28, 1937.
- Rossby, C. G., On the mutual adjustment of pressure and velocity distributions in certain simple current systems. part ii, *J. Mar. Res.*, 1, 239–263, 1938.
- Sielecki, A., An energy-conserving numerical scheme for the solution of the storm surge equations, *Mon. Weather Rev.*, 96, 150–156, 1968.
- Smolarkiewicz, P. K., A simple positive definite advection scheme with small implicit diffusion, *Mon. Wea. Rev.*, 111, pp. 479, 1983.
- Yoshida, K., A theory of the Cromwell current and of equatorial upwelling, *J. Oceanogr. Soc. Japan*, 15, 154–170, 1959.